Study on forming control and penetration performance of tantalum in linear explosively formed penetrators (LEFP) warhead

H Deng*, G Li, Z Liang, X Ren, H Guo
Xi'an Modern Chemistry Research Institute, Xi'an, Shaanxi, China

ABSTRACT
In order to further improve the penetration power of the multi-explosive formed warhead, tantalum is used to design a multi-explosive folded warhead. Firstly, using numerical simulation, the design parameters of the damage element of two different forming methods are obtained. Then the formation process, flight process, and penetration process of the projectile were calculated respectively. Finally, the static explosion experiment of the warhead was carried out. The results show that the calculated results are in good agreement with the experimental results. There was no break during the formation of the penetrator. It can be folded to form a rod-shaped penetrating body with a high aspect ratio, which can penetrate a Q235 steel target with a thickness of 30mm at a distance of 3 meters. Tantalum material is used as a shaped charge liner, which has a much higher penetration power and stronger aftereffect than copper and pure iron.

1. INTRODUCTION

Explosively formed projectile (EFP) has the characteristics of high explosive height, large mass and high efficiency. Compared with traditional fragments, EFP has certain advantages in impact speed and specific kinetic energy. In the field of air defense and antimissile, EFP can intercept targets with large wall thickness, such as tactical ballistic missile (TBM), but its application is limited due to the small number of damage elements [1]. In order to increase the integrated quantity of liner and ensure its damage power, the circumferential linear explosively formed projectile (MLEFP) was developed. The technical method is to place the liner in the circumferential direction of the charge and integrate a large number of charge liners. When the charge is detonated, the liner will overturn under the effect of detonation pressure, forming a linear explosively formed penetrating body of a certain length on the symmetry plane, which has high speed, high kinetic energy, high hit rate and higher penetration power [2-4].

The density, strength and plastic state of liner material will directly affect the forming and penetration performance of EFP. Pure tantalum has a density of 16.7g/cm^3 and an elongation rate of 60%. and it has the properties of high ductility, high sound velocity and high melting point, so its physical and mechanical properties can meet the material performance requirements of shaped charge liner. Compared with red copper, the tensile length of the penetrator formed by tantalum shaped charge liner is greatly increased [5,6].

*Corresponding Author: hai179590@163.com

Some studies show that the penetration depth of tantalum EFP is increased by 55.4% compared with that of red copper, and the penetration power is greatly improved [7,8].At present, research on tantalum as liner material has become a research hotspot, Weimann [9] compared the penetration power of tantalum and iron EFP, and concluded that the damage ability of tantalum EFP with aspect ratio of 3 is equivalent to that of iron EFP with aspect ratio of 6 under the same mass. Biass [10] compared and studied the penetration ability of cavity tantalum EFP, dense tantalum EFP and optimized iron EFP. The results show that the penetration ability of cavity and dense tantalum EFP is increased by 14.2% and 34.9% respectively. Guo Teng-Fei [11] studied the influence of structural design parameters of tantalum cover on the shaping and penetration performance of EFP and obtained a better combination of structural parameters. Li Peng [12] studied a rod-type circumferential multi-explosive-formed projectile warhead. The liner material is pure iron. Through numerical simulation and experimental verification, a compact projectile with an aspect ratio of 4:1 can be penetrated. 30mm Q235 steel plate.

The above researches mainly focus on the design of EFP forming parameters and the application of tantalum in traditional EFP liner. There are few reports on the molding control and research of tantalum in linear EFP [13-16]. In order to further improve the damage power and the number of damage elements, this paper designs a new type of circumferential multi-linear explosively formed projectile (MLEFP), which uses tantalum as the liner material , and through the molding control, the rod shaped damage element with large length diameter ratio is formed, which improves the penetration power and hit accuracy of the damage element, and provides design support for the design of air defense and antimissile warhead.

2. LEFP WARHEAD DESIGN

The warhead is composed of a fully prefabricated strip shaped charge liner, a shell, an end cover and a charge. The caliber of the warhead is 127mm, and the initiation mode is center initiation. The structure diagram of the warhead is shown in Fig.1. The liner is an arc-shaped liner with variable wall thin at the middle and thick at both ends. By adjusting the change of wall thickness, the damage element is controlled to be folded and formed. The length of the liner is 100 mm, the mass is 74g, the quantity is 36 pieces, the material is tantalum, the end cover and shell are hard aluminum, the charge is B explosive.

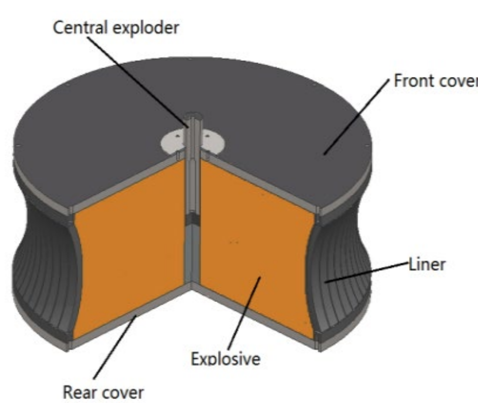

Fig.1 Structure diagram of warhead

3. NUMERICAL SIMULATIONS

The autodyn-3D software is used for numerical simulation. Since the warhead is a centrosymmetric structure, only 1/4 model is established in the calculation, and the calculation model is shown in Fig.2. ALE structured grid is used for liner, shell and end cover components, and Euler algorithm is used for charge and air area. The interaction among explosive, liner, air and shell adopts fluid-structure coupling algorithm. Lagrangian velocity tracking points are set on one of the liners to record the velocity distribution of each point on the liner when the explosive stops working.

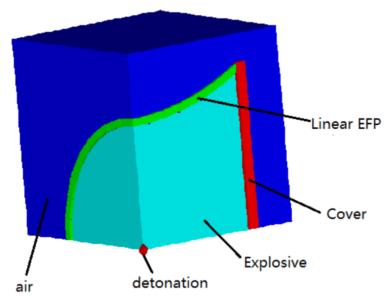

Fig.2 Calculation model

In the calculation process, the B explosive adopts the JWL equation of state, and the parameters are the parameters of the AUTODYN software; the state equation of the tantalum material adopts the Shock model, and the state equation is the Mie–Grüneisen equation:

$$p = \frac{\rho_0 C^2 \mu[1+(1-\frac{\gamma_0}{2})\mu-\frac{\alpha}{2}\mu^2]}{[1-(S_1-1)\mu-S_2\frac{\mu^2}{\mu+1}-S_3\frac{\mu^3}{(\mu+1)^2}]^2} + (\gamma_0+\alpha\mu)E \tag{1}$$

Where: ρ_0 is the initial density of the material; E is the internal energy; $C, S_1, S_2, S_3, \gamma_0, \alpha$ are the material characteristic parameters; $\mu = \rho/\rho_0 - 1$, ρ is the material density corresponding to the current time step, and the parameters are shown in Tab 1. The material constitutive model is taken as the Johnson-Cook model, [17-20], and its structural expression is:

$$\sigma = (142 + 164\varepsilon^{0.3148})(1 + 0.057\dot{\varepsilon}*)(1 - T^{*0.8836}) \tag{2}$$

Where: σ is the flow yield strength of the material; ε is the equivalent plastic strain; $\dot{\varepsilon}*$ is the dimensionless equivalent plastic strain rate; T^* is the dimensionless temperature.

Table.1 Parameters of tantalum

C	γ_0	S_1	S_2	S_3	$\rho/(g\cdot cm^{-3})$
0.341	1.99	1.2	0	0	16.6

3.1 optimization design of liner structure parameters

After optimization design, a kind of structure parameters which can be formed into double fold damage element is determined. The thinnest part in the middle is 5mm, the thickest part at both ends is 7mm, the inner arc radius is 80mm, and the outer arc radius is 65mm.

Fig.3 shows the dispersion effect of damage elements after warhead model explosion. It can be seen that damage elements are evenly distributed on the central plane of warhead and scattered on the same circle with warhead axis as the center. It shows that the velocity direction of damage elements formed is perpendicular to the axis of warhead and the velocity between damage elements is the same. The radial scattering velocity curve of the damage element is shown in Fig.5(a). After 0.008 ms initiation, the damage element starts to fly outwards. Under the action of detonation products and detonation waves, the velocity first increases sharply. With the increase of time, the change rate of the velocity rise decreases continuously. After 0.03 ms, the velocity reaches the maximum value, the maximum value is 1311 m/s, after which it will remain unchanged and fly outwards.

The explosive forming process of damage element is shown in Fig.4. Due to the change of liner wall thickness and radial charge thickness, the axial loading ratio of each element changes continuously. When the liner is driven by detonation, there are velocity gradients among the micro elements in the axial direction, and the liner turns over and folds, resulting in two-fold penetrators. The velocity curve of the liner closure is shown in Fig.5 (b). It can be seen that the closure velocity of the damage element increases sharply during the 0.03 ms explosion period, and the maximum closure velocity is 275 m/s. After the explosive effect of the explosive is over, the velocity gradient of each element in the axial direction of the charge type cover is continuously reduced, and the closing speed also decreases. After 0.126 ms, the closing velocity decreases to 0, and the damage element is closed and formed into a dense double folded rod penetrator. The length, thickness and width of the penetrator are 27.8 mm, 11.8 mm and 15.1 mm respectively.

The explosive forming process of damage element is shown in Fig.4. Due to the change of liner wall thickness and radial charge thickness, the axial loading ratio of each element changes continuously. When the liner is driven by detonation, there are velocity gradients among the micro elements in the axial direction, and the liner turns over and folds, resulting in two-fold penetrators. The velocity curve of the liner closure is shown in Fig.5(b). It can be seen that the closure velocity of the damage element increases sharply during the 0.03 ms explosion period, and the maximum closure velocity is 275 m/s. After the explosive effect of the explosive is over, the velocity gradient of each element in the axial direction of the charge type cover is continuously reduced, and the closing speed also decreases. After 0.126 ms, the closing velocity decreases to 0, and the damage element is closed and formed into a dense double folded rod penetrator. The length, thickness and width of the penetrator are 27.8 mm, 11.8 mm and 15.1 mm respectively.

Fig.3 Dispersion process of damage element

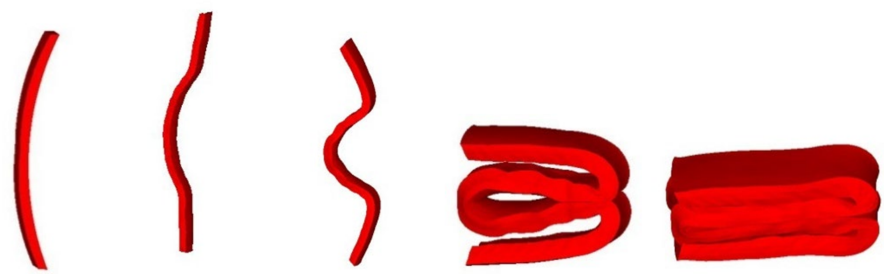

Fig.4 Forming process of damage element

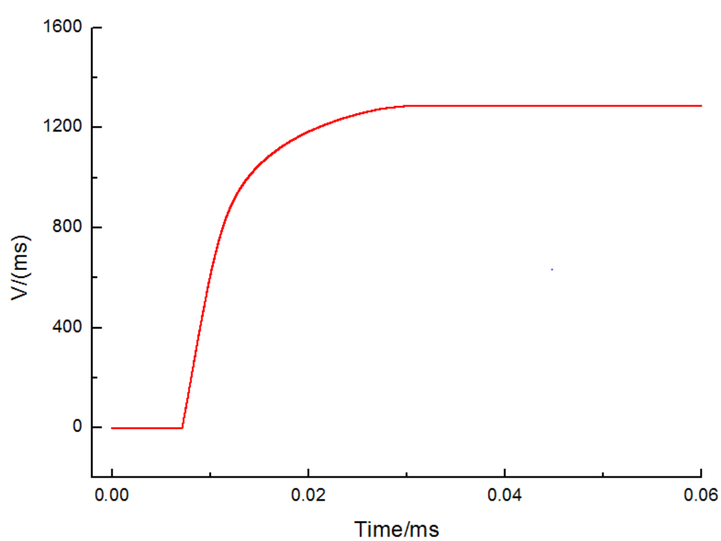

(a) Dispersion speed of damage element

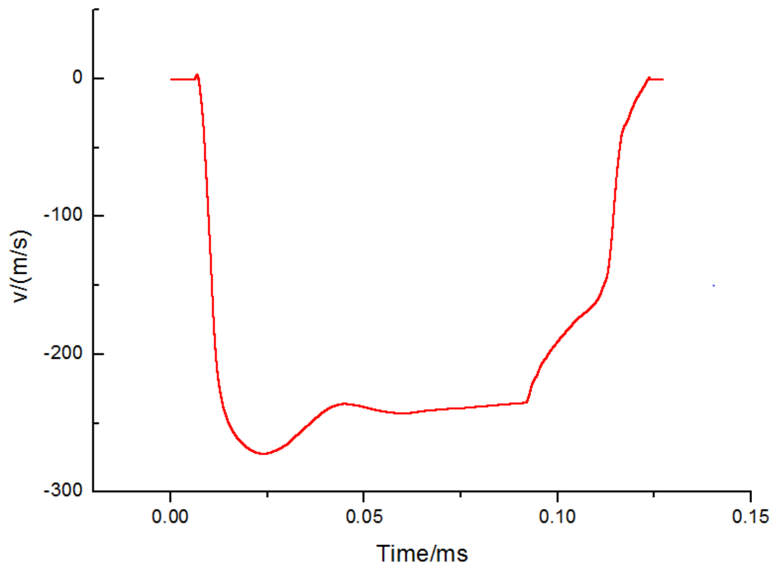

(b) Closing speed of damage element

Fig.5 Speed curve

After optimization and adjustment, the parameters of the liner which can be formed into a single fold damage element are determined as follows: the span is 80mm, the thinnest part in the middle is 4mm, the thickest part at both ends is 7.5mm, the inner arc radius is 80mm, the outer arc radius is 68mm. After numerical simulation, the dispersion effect of the warhead model after explosion is shown in Fig.6. It can be seen that the damage elements are evenly distributed on the central plane of the warhead and on the same circle with the warhead axis as the center, indicating that the velocity direction of the damage elements formed is vertical to the warhead axis, and the velocity between the damage elements is the same. The radial dispersion velocity curve of the damage element is shown in Fig.6(a). The damage element starts to disperse outward at 0.008 ms after initiation. Under the action of detonation products and detonation waves, the velocity first increases sharply, and the increase rate decreases with time. After 0.028 ms, the velocity reaches the maximum value, which is 1337 m/s, and then keeps unchanged.

The explosive forming process of damage element is shown in Fig.7. Due to the change of liner wall thickness and radial charge thickness, the axial loading ratio of each element changes continuously. When the liner is driven by detonation, there are velocity gradients among the micro elements in the axial direction, and it turns over and folds, and finally turns over and folds to form the penetrator. The velocity curve of the liner closure is shown in Fig.8(b). During the 0.03ms explosion period, the closure velocity of the damage element increases sharply, and the maximum closure velocity is 178 m/s. After the explosion, the velocity gradient decreases continuously, and the closure velocity also decreases. After 0.137 ms, the closure velocity decreases to 0, and the damage element is closed into a dense double folded rod penetrator. The length of the penetrator is about 41.67mm, the maximum width is 15.7mm and the maximum thickness is 8.26mm.

Fig.6 Damage element dispersion process

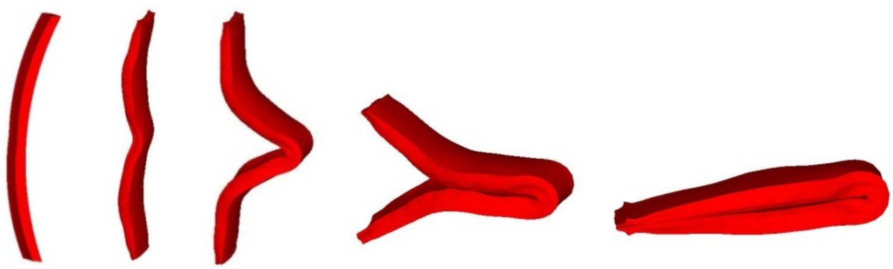

Fig.7 Damage element forming process

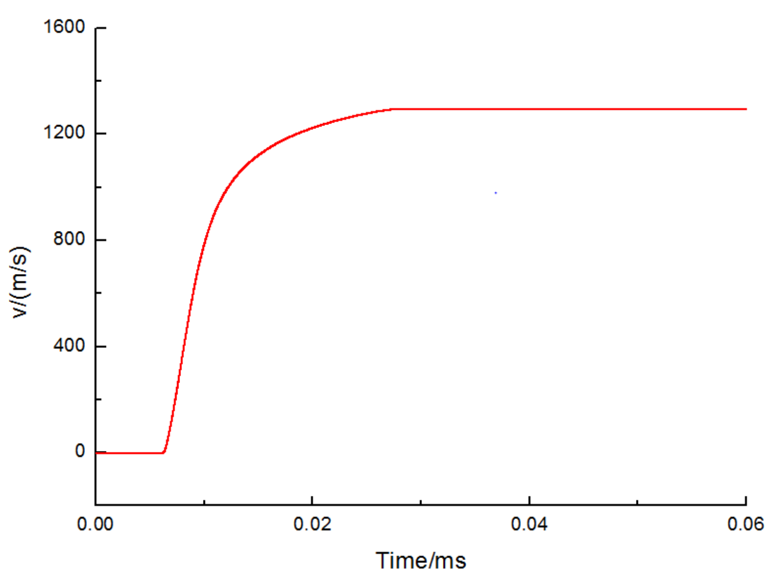

(a) Dispersion speed of damage element

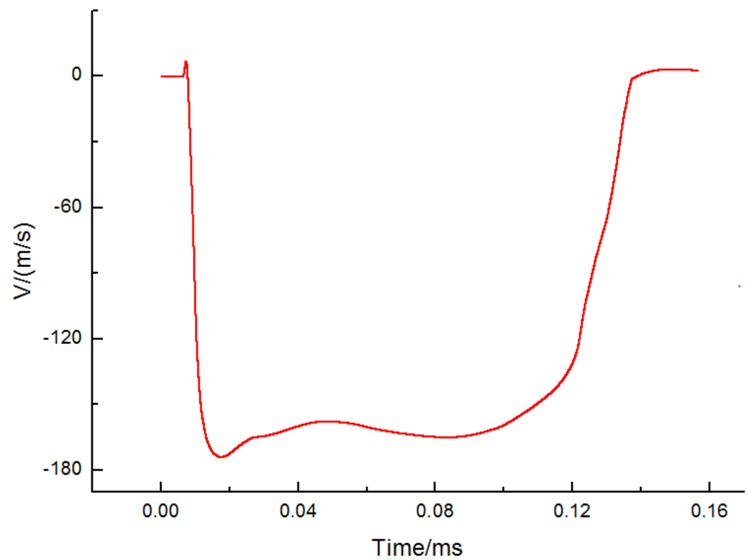

(b) Closing speed of damage element

Fig.8 Velocity curve

3.2 penetration process of damage element

According to the size of shaped rod damage element obtained by numerical calculation, the models of one-fold and two-fold penetrator are established respectively. The length of two-fold penetrator is 27.8 mm, the width is 15.1 mm, the thickness is 11.8 mm, and the velocity of the penetrator is 1311 m/s; the length of one fold penetrator is 41.67 mm, the width is 15.7 mm, the thickness is 8.26 mm, and the velocity of the penetrator is 1337 m / s. The target is 120mm long, 120mm wide, and 30mm thick. The target is set with boundary conditions, using the JC failure model, and the material's erosion factor is 1.1.

The penetration process of the damage element is shown in Fig.9 and Fig.10. It can be seen that the two kinds of penetrators can completely penetrate the target plate, the penetration holes are relatively regular, there are flanging in the front of the target plate, and the back of the target plate forms some collapses due to the effect of tensile wave. Firstly, the damage element penetrates the target plate at a high speed, forming a plastic deformation area in the contact area and forming an extrusion hole. As the penetration depth of the damage element increases, the damage element is constantly eroded, and the shear band and tensile section are formed in the target [21-24]. Finally, when the non-penetrated part of the target is thin enough, under the action of the residual kinetic energy of the damage element and the reflected shock wave from the back, the target is washed out, forming a collapse and flying out together with the residual damage element [25].

Through the comparison of the penetration process of two kinds of damage elements, the damage element formed by one-fold has a longer residual length after penetrating the target plate, and also has the penetration ability of penetrating the thicker target plate; the damage element formed by two fold has been almost completely eroded and worn after penetrating the target plate, and has no penetration ability of penetrating the thicker target plate.

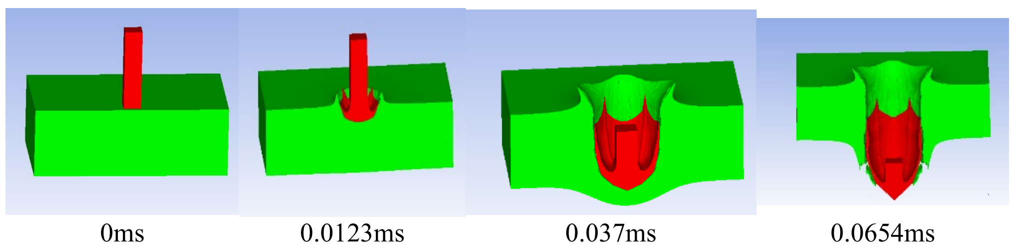

Fig.9 Penetration process of one-fold shaped damage element

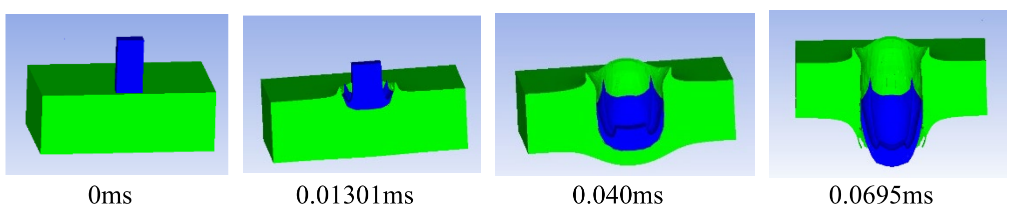

Fig.10 Penetration process of two-fold shaped damage elements

4. EXPERIMENTAL VERIFICATION

4.1 Test Layout

According to the optimized structural parameters of one-fold forming damage element, a prototype with a diameter of 127 mm and a length of 140 mm is processed. The charge is explosive B, and 36 fully prefabricated linear EFPs are distributed circumferentially. The prototype is shown in Fig.11 (a). One Q235 power target with thickness of 20 mm and 30 mm is set at 2 m away from the blasting center. Two 20 mm thick pmx-2 shielding charges are arranged at a distance of 2 m from the detonation center, and a velocity measuring target is arranged on the power target to test the impact velocity of the damage element. The test layout is shown in Fig.11(b).


(a) Principal prototype

(b) Test layout

Fig.11 Test prototype and test layout

4.2 Test Results

The distribution and perforation results of the damage elements after penetrating the target plate are shown in Fig.12. The white holes are the penetration holes of the warhead prototype. It can be seen that all the Q235 power targets of 20mm and 30mm are penetrated. The distribution of the penetration holes is almost on the same horizontal line, and the average spacing between the two is 34cm. The linear density of the damage elements at 2m away from the detonation center is 3.9 per meter. The shape of the penetration hole is regular, almost circular, with an average diameter of 3.1cm on the front and 2.8cm on the back. Along the thickness direction of the target plate, the diameter of the hole decreases to a certain extent. Tantalum erosion can be observed on the hole wall of the target plate. The target plate is crushed by the penetrator, and there is a certain mass loss in the process of penetration.

Through the penetration effect of the damage element, it can be concluded that the tantalum shaped charge damage element does not break during the explosive forming process, and it is folded to form a dense rod penetrator, which has a good flight attitude and penetration ability. The velocity of the damage element measured in the experiment is 1281 m/s, and that of the numerical simulation is 1326 m/s, with a difference of 3.6%, which is basically consistent with the experimental data. The error may be caused by the simplification of the calculation model and the selection of relevant parameters.

(a) Perforation of 20 mm target plate

(b) Perforation of 30 mm target plate

Fig.12 Penetration result of damage element into power target

5. CONCLUSIONS

(1) Tantalum material has good ductility and will not be broken during explosive forming. The spherical zonal liner with a wall thickness difference of 4mm can be folded to form rod penetrator, and the aspect ratio is about 4:1;

(2) The shape, distribution, velocity and penetration process of the damage elements formed in the explosively formed warhead are consistent with the numerical simulation results. The damage element can fly evenly along the axis of the vertical warhead, and can penetrate the Q235 steel target of 20 mm and 30 mm at a distance of 2 meters from the detonation center. Compared with copper and pure iron, the penetration power of the damage element is greatly improved.

REFERENCE

[1] Yin Jian-Ping, Wang Zhi-Jun, Xiong Yong-Jia, et al. Effect of curvature radius of liner on circumferential mlefp forming [J]. Chinese Journal of Explosives and Propellants, 2013, 21(4):512-516.

[2] Cardoso D., Teixcira-Dias F. Modelling the formation of explosively formed projectiles (EFP) [J]. International Journal of impact Engineering, 2016, 93:116-127.

[3] Huang Xian-Ning, Li Wei-Bing, Cheng Wei. Feasibility of cone arc combined with cover shaped rod shaped dense EFP [J]. Chinese Journal of Energetic Materials, 2019, 27 (2): 90-96.

[4] Zhu Xu-Qiang, Wang Feng, Du Zhong-Hua. Study on forming mechanism and penetration power of multimode LEFP [J]. Chinese Journal of Explosives and Propellants, 2016, 39 (4): 61-68.

[5] Peng Hai-Jian, Yan Xiao-Dong, Li Defu. Application of tantalum in armor piercing ammunition liner [J]. Journal of Rare metals, 2006, 30 (5): 678-681.

[6] Ya-Jun Wang, Wei-Bing Li, Wen-Bin Li, et al. Influence of Structural Characteristics on EFP Formation Under Different Liner Materials [C]. Conference: 31st International Symposium on Ballistics, INDIA, November 2019:4-8.

[7] Han Wei, He Yong, Shen Xiao-Jun. Research on EFP forming and penetration of zirconium tantalum composite liner [J]. Journal of Ordnance Equipment Engineering, 2019, 40 (4): 163-168.

[8] Fan Xue-Fei, Li Wei-Bing, Wang Xiao-Ming, Simulation and experimental study on formation of dual mode damage element in tantalum liner driven by detonation [J]. Acta Armamentarii. 2017,38 (10): 1918-1923.

[9] Wei M K., BiacheI A. Terminal ballistics of EFPs with high L/D-ratio [C], 17th International Symposium on Ballistics, Midrand, South Africa, 1998:215-224.

[10] Biass S, Todde A, Cioni R, et al. Potential impacts of tephra fallout from a large-scale explosive eruption at Sakurajima volcano [J]. Journal of Bull Volcanol (2017) 79:73.

[11] Guo Teng-Fei, Li Wei-Bing, Li Wen-Bin, et al. Effect of structural parameters of tantalum cap on EFP forming and penetration performance [J]. Journal of high pressure physics, 2018,32 (3): 104-110.

[12] Li Peng, Yuan Bao-Hui, Li Gang, et al. Research on the Warhead Numerical Simulation of a Rod Type Circumferential Multiple Explosively Formed Projectile [J]. Journal of missiles and guidance, 2017,37 (1): 70-76.

[13] Zhe Wang,Jian-Wei Jiang,Shu-You Wang,et al. Jet Formation and Penetration Study of Double-Layer Shaped Charge [J]. Journal of Energetic Materials.2018,36(2).152-168.

[14] Kim H J, Yi Y S, Park L J. Analysis of forming characteristics of Ta EFP according to material model [J]. EFP Web of Conferences, 2015, 94:40-60.

[15] Luo Jian-Hua. Research on compact tantalum alloy EFP warhead [D]. Nanjing: Nanjing University of technology, 2018:1-62.

[16] Han Wei, He Yong, Shen Xiaojun. Research on EFP forming and penetration of zirconium tantalum composite liner [J]. Journal of Ordnance Equipment Engineering, 2019, 40 (4): 163-169.

[17] Jia Zi-Jian, Wang Zhi-Jun, Yi Jianya. Jet forming and penetration simulation of double-layer liner with central hole [J]. Journal of missile and guidance. 2018, (4). 28-32.

[18] Zhao Li-Jun, Zhu Xiao-Ping, Yin Long, et al. Numerical simulation and experimental study on armor breaking power of different material liner [J]. Weapon material science and engineering. 2018, (1). 89-92.

[19] Li W B, Wang X M. et al. Effect of the liner material on the shape of dual mode penetrators [J]. Combustion, Explosion and Shock Waves, 2015, 51(3): 387-394.

[20] Cardoso D., Teixeira-Dias F. Modelling the formation of explosively formed projectiles [J]. International Journal of Impact Engineering, 2016, 93: 116-127.

[21] Zhu Zhi-Peng, Men Jian-Bing, Jiang Jian-Wei. Research on control of large aspect ratio tantalum explosively formed projectile [J]. Acta Armamentarii, 2018, 39 (1): 30-38.

[22] Han Wei, He Yong, Shen Xiao-Jun, et al. Study on EFP forming and penetration of zirconium tantalum composite liner [J]. Journal of ordnance and equipment engineering. 2019, (4). 163-167173.

[23] Sun Jia-Xiao, Yin Jian-Ping, Wang Zhi-Jun, et al. Study on orthogonal design of three factors: long short axis ratio, acoustic impedance of aluminum, copper and iron and cover spacing during charge jet forming of double-layer elliptical charge liner [J]. Journal of ordnance and equipment engineering. 2016, (6). 135-139.